/

Article / Book Information

Title	Apparent zeta potential of nano-porous Al2O3 film deposited on different substrates in streaming potential method
Authors	Akio Sayano, Tadashi Shiota, Akio Nishiyama, Kouichi Yasuda, Kazuo Shinozaki
Citation	Journal of Materials Science, Vol. 53, Issue 24, pp. 16232-16242
Pub. date	2018, 8
Note	This is a post-peer-review, pre-copyedit version of an article published in Journal of Materials Science. The final authenticated version is available online at: http://dx.doi.org/10.1007/s10853-018-2791-5.

Ceramics

CrossMark

Apparent zeta potential of nano-porous Al$_2$O$_3$ film deposited on different substrates in streaming potential method

Akio Sayano[1,*] , Tadashi Shiota[1], Akio Nishiyama[1], Kouichi Yasuda[1], and Kazuo Shinozaki[1]

[1] School of Materials and Chemical Technology, Tokyo Institute of Technology, Meguro-ku, Tokyo 152-8550, Japan

ABSTRACT

Al$_2$O$_3$ films were coated on SUS304L stainless steel and fused silica substrates using chemical solution deposition. Continuous pores with a diameter of approximately 2 nm were observed through the measurement of the pore diameter distribution in the Al$_2$O$_3$ films using N$_2$ gas adsorption. The zeta potential of the Al$_2$O$_3$ film was measured using the streaming potential method, and the effect of the substrate material on the zeta potential was investigated. Initially, the measured zeta potential of the Al$_2$O$_3$ films was + 40 to + 50 mV, which was the same for both the SUS304L and fused silica substrates. However, the zeta potential of the Al$_2$O$_3$ film on the fused silica substrate decreased significantly with repeated measurements. Elemental analysis of the Al$_2$O$_3$ film in the depth direction using dynamic secondary ion mass spectroscopy showed that both K and Cl contents increased after zeta potential measurements were taken. Moreover, the zeta potential of a specimen impregnated with KCl electrolyte solution under vacuum exhibited no dependence on the number of measurements taken. It was thereby considered that the decrease in the zeta potential with repeated measurements was caused by the gradual penetration of the electrolyte solution into the pores, which eventually reached the fused silica substrate. This is a characteristic phenomenon observed when the zeta potential of a film that contains continuous pores is measured using the streaming potential method.

Introduction

Solid particles in a fluid can deposit and accumulate on the components of equipment and systems that employ fluids, such as nuclear power plants, and obstruct the flow of the fluid. As a result, the performance of the equipment or system may be degraded, and damage to the equipment may result. Therefore, there is a demand for technology to suppress the deposition of solid particles in fluids on the components [1–3].

Address correspondence to E-mail: sayano.a.aa@m.titech.ac.jp

Zeta potential control is a method to suppress the deposition of solid particles onto the surfaces of parts. In this method, a film with the same zeta potential sign as that of the solid particles in the fluid is coated on the components, thereby creating a repulsive force between the solid particles in the fluid and the component surface [1–6]. This is a unique and excellent method that takes advantage of the intrinsic characteristics of the material and does not consume energy to suppress deposition.

The chemical solution deposition (CSD) method considered in this study is a well-established practical process to coat large parts [7–11]. In the CSD method, a ceramic film is formed on a substrate by first depositing a ceramic precursor solution on the substrate surface and then applying heat treatment to decompose the precursor. This process is advantageous in that it does not require special equipment and is applicable to large parts with complex shapes. However, films formed using CSD typically have a characteristic microstructure with continuous pores [22–24].

Many of the large parts that are considered in this study are metallic. Therefore, accurate measurement of the zeta potential of a film containing continuous pores that is coated on a metal substrate is necessary. Electrophoresis is also commonly used to evaluate zeta potential, but this method involves the application of a high voltage to the electrolyte solution and is therefore difficult to use in electrically conductive substrate [13]. The streaming potential method [12] can be used to measure the zeta potential of a film coated on a metal substrate. In the streaming potential method, an electrolyte solution is passed between two specimens placed on either side of a narrow gap and the resulting voltage or current is measured. A voltage is not applied in this procedure, and thus, evaluation of the zeta potential of a film on a metal substrate should be possible. This method requires the application of pressure to move the electrolyte solution. As a result, the electrolyte solution may penetrate the pores of the film, resulting in interactions between the electrolyte solution and the substrate that could affect the measured zeta potential.

Very few reports discuss the zeta potential of a film containing continuous pores that is coated on a metal substrate by the use of the streaming potential method to measure. Lorenzetti et al. [14] coated a TiO_2 film with a thickness of 30 μm on a Ti metal substrate via a hydrothermal method using a Ti alkoxide precursor, and then evaluated the zeta potential using the streaming potential method. Specifically, they measured the electrical conductivity between the electrodes for different gap distances between the specimens. They concluded that the streaming current flows in the pores in the film, according to data extrapolated to zero gap distance. Moreover, they corrected these data to obtain accurate zeta potential. However, the film investigated in their study was relatively thick (approximately 30 μm), and they did not consider the interaction between the electrolyte solution that penetrated the film pores and the substrate. Daiguji et al. published a related report on the behavior of electrolyte solution in a SiO_2 nanotube. They placed a KCl electrolyte solution at both ends of a SiO_2 nanotube with a diameter of 30 nm and a length of 5 μm, and then analyzed the behavior of the K^+ and Cl^- ions using a two-dimensional continuum equation [15]. They concluded that K^+ ions penetrated the nanotube, but Cl^- ions were unable to penetrate because the SiO_2 nanotube surface was negatively charged in the KCl electrolyte solution. However, these results do not consider any pressure difference and therefore are not applicable in cases where pressure is applied, such as the streaming potential method.

Determining whether the substrate has any effect on the zeta potential of the film is important to accurately measure the zeta potential of a film with continuous pores on a metal substrate. To this end, stainless steel and fused silica were chosen as substrates. An Al_2O_3 film was coated on these substrates using CSD, and the differences in the zeta potentials of these specimens were examined by the streaming potential method.

This report investigates for the first time the effect of substrate type on the zeta potential of films coated on the substrate. Furthermore, the origin of the decrease in zeta potential with repeated measurements, a phenomenon discovered during the investigation, is discussed.

Materials and methods

Film formation

The substrates used in this study were SUS304L [composition: C (0.021%), Cr (18.15%), Ni (9.06%), Mn (0.98%), Si (0.64%), P (0.031%), and S (0.004%)] and

fused silica (ES, Tosoh Quartz). The substrate was in the form of a rectangular plate, and the arithmetic average roughness, Ra, was approximately 0.4 μm.

An Al_2O_3 film was coated onto each substrate using CSD. Figure 1 depicts the film preparation process. Both substrates were ultrasonically cleaned in acetone, immersed in an Al_2O_3 solution, diluted to the specified concentration using pure water, and then removed at a fixed rate of 2 mm s^{-1}. Pseudo-boehmite sol was used as the Al_2O_3 sol (10A, Kawa-ken Fine Chemicals) and was obtained by the hydrolysis of Al alkoxide. After dip-coating, the specimens were dried at room temperature and heat-treated in an electric furnace at 773 K for 30 min in air at the rate of 10 K min^{-1}. Subsequently, the speci-mens were cooled in the furnace. The film thickness was controlled by repeating the above procedure. Heat treatment conditions of 773 K and 30 min were determined to allow for the complete thermal decomposition of the Al_2O_3 sol.

A self-supporting film was prepared using the same Al_2O_3 sol in order to investigate the properties of this film. A silicone resin mold (inner dimensions: diameter 60 mm × height 15 mm) was placed on a plate of glass that had been coated with a 50-μm-thick fluoropolymer layer. The Al_2O_3 sol described above was poured into the mold and dried at 333 K for 5 h. The obtained thin film was placed in a mullite cru-cible, and heat treatment was carried out under the same conditions used to prepare the coated films described above. A self-supporting film with a thickness of approximately 80 μm was obtained.

Evaluation
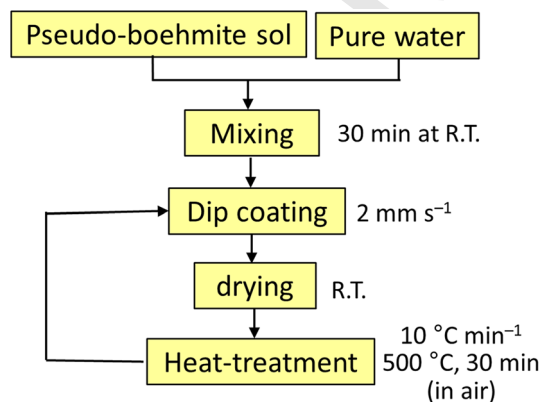
A specimen (dimensions $10 \times 20 \times 1$ mm^3) was prepared with an Al_2O_3 film coating on a fused silica substrate using the process described above. The specimen was embedded in resin, and the resulting material was cut through the middle and polished using waterproof abrasive paper. The cross-sectional region of the coating was then machined using an ion beam (SM09010CP, JEOL). The obtained cross section of the coating was observed using a field emission scanning electron microscope (FE-SEM; S-4700, Hitachi).

The zeta potentials of the Al_2O_3 films coated on the substrates were measured using the streaming potential method (SurPASS^{TM} 3, Anton Paar). Fig-ure 2 shows a schematic of the zeta potential mea-surement by the streaming potential method. A pH of approximately 5.5 was maintained during the mea-surements by bubbling N$_2$ gas through the electrolyte solution, as needed. The measurement temperature was approximately 300 K, the electrolyte was a 1 mM solution of KCl, and the gap between the samples was approximately 100 μm. The pressure was increased to a maximum of approximately 50000 Pa, but the zeta potentials were calculated based on the streaming current in the stable range of 20000–38000 Pa using the following Helmholtz–Smolu-chowski equation [16],

$$\zeta = \mathrm{d}I/\mathrm{d}P \times \eta/\varepsilon\varepsilon_0 \times L/A \tag{1}$$

where ζ is the zeta potential, I is the current, P is the pressure, η is the viscosity of electrolyte, ε is the rel-ative permittivity, ε_0 is the permittivity of vacuum, L is the channel length, and A is the cross-sectional area of channel. A polypropylene (PP) film with a thick-ness of 50 μm was placed opposite to the coated
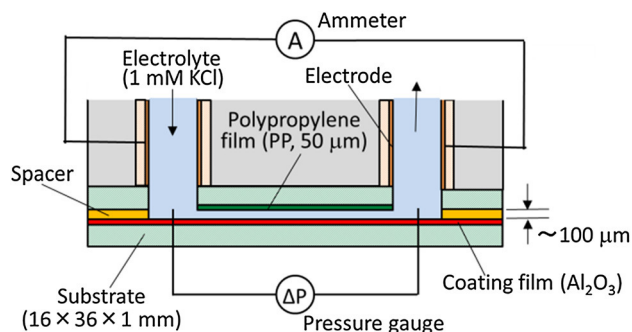

Figure 1 Procedure for preparing films.

Figure 2 Schematic illustration of the testing apparatus for zeta potential by streaming potential method.

specimen to be measured. Therefore, the apparent
zeta potential obtained in the measurements was the
average of the values for the coated specimen and PP.
The zeta potential of the coated specimen was
derived using Eq. (2) below. The zeta potential of PP
(23.5 mV) was obtained beforehand using the same
conditions and equipment, by placing two PP films
opposite to each other.

$$\zeta_m = 1/2 \times \zeta + 1/2 \times \zeta_p$$
$$\zeta = 2 \times \zeta_m - \zeta_p \qquad (2)$$

where ζ_m is the measured zeta potential, ζ is the zeta
potential of specimen, and ζ_p is the zeta potential of
PP. Measurements were repeated six times to verify
the reproducibility of the data.

The pore distribution of the Al_2O_3 film was ana-
lyzed using gas adsorption measurements (Autosorb-
1, Quantachrome). Plate-shaped fused silica and
SUS304L specimens (dimensions: $22 \times 5 \times 1$ mm^3)
were coated using the above process. Seven Al_2O_3
films, total weighing 8–9 mg, were prepared for
testing. The N_2 adsorption isotherm at 77 K was
measured, and the pore distribution of the film was
evaluated using the Barrett–Joyner–Halenda (BJH)
method [17]. A similar measurement was taken for a
self-supporting Al_2O_3 film weighing 173 mg. In
addition, the true density of the self-supporting
Al_2O_3 film was determined by helium displacement
using Archimedes' principle. The film pore ratio p is
defined as

$$p = v/(v + (1/d)) \times 100 \qquad (3)$$

where d is the true density and v is the total pore
volume that can be determined by pore distribution
analysis.

Results and discussion

Film characterization

Figure 3 shows an example of a cross-sectional FE-
SEM image. In this case, the Al_2O_3 film was coated by
single immersion in 6.7 wt.% Al_2O_3 sol. The film was
firmly attached to the substrate. The thickness of the
film was approximately 0.5 μm, and the weight of the
film per unit surface area was 1.04 g m^{-2}, as derived
from the change in weight after coating and the
specimen surface area. Subsequent film thicknesses
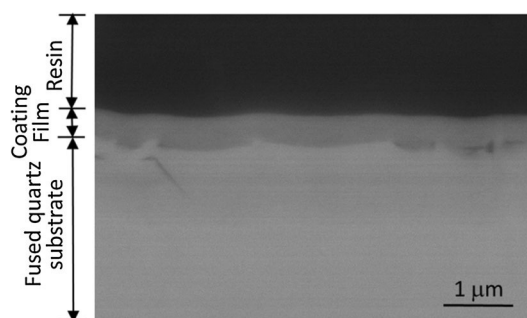were calculated using the weight change after

Figure 3 FE-SEM image of the cross section of an Al_2O_3 film
coated on a fused silica substrate.

coating, assuming that the weight of the film per unit
surface area was proportional to the film thickness.

Figure 4 shows the relationship between the
number of dipping cycles and the film thickness for
the SUS304L and fused silica substrates. The alumina
sol concentration was 6.7 wt.%, and the dimensions
of the specimens were $16 \times 36 \times 1$ mm^3. The film
thickness increased linearly with the number of dip-
ping cycles for both substrates. There was no signif-
icant difference in the manner in which the Al_2O_3 sol
deposited on these substrates.

Figure 5a shows the pore diameter distribution of
Al_2O_3 films coated on SUS304L and fused silica
substrates, and that of a self-supporting Al_2O_3 film.
Figure 5b plots the cumulative pore volume of the
Al_2O_3 film coated on a fused silica substrate. The pore
diameter distribution showed a sharp peak at about
2 nm in all cases, demonstrating that the Al_2O_3 films
in this study had pores with a uniform diameter of
approximately 2 nm. The cumulative pore volume of
the Al_2O_3 film on a fused silica substrate was
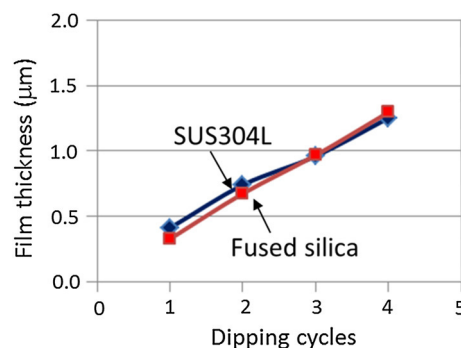0.33 cm^3 g^{-1}, and the true density of self-supporting

Figure 4 Relationship between number of dipping cycles and
thickness of Al_2O_3 films coated on SUS304L and fused silica
substrates (sol: pseudo-boehmite 6.7 wt.%, treatment: 500 °C,
30 min).

Figure 5 **a** Pore diameter distribution for Al_2O_3 films coated on substrates and self-supporting Al_2O_3 film. **b** Cumulative pore volume for Al_2O_3 film coated on a fused silica substrate.
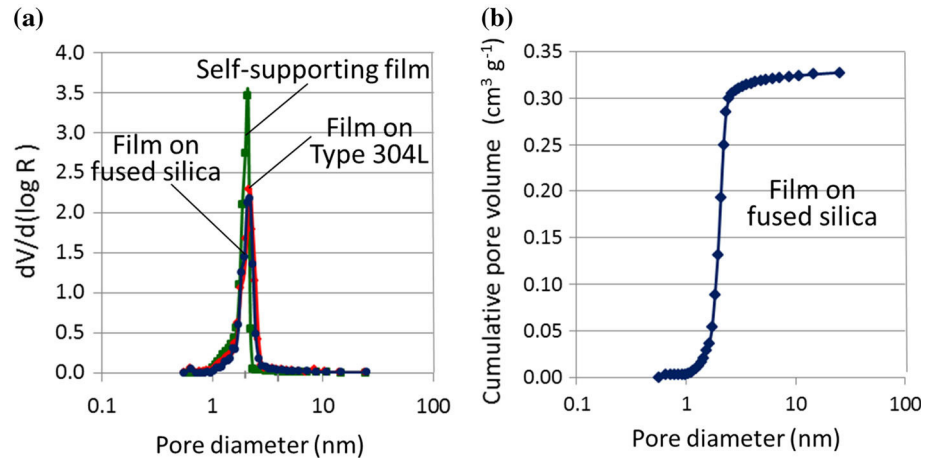
film, as determined by helium displacement using Archimedes' principle, was 3.01 g cm^{-3}. The porosity of the Al_2O_3 film coated on a fused silica substrate was 50%, assuming that the true density of the Al_2O_3 film was the same for the film on the substrate and the self-supporting film. The microstructure of the Al_2O_3 film in this study was determined to consist of small pores, with a high porosity.

Guo et al. [22] formed a Nb_2O_5 film on electrically conductive glass by CSD using $NbCl_5$ as the raw material; then, they measured the pore diameter using N_2 adsorption. They found that the pore diameter varied widely (from 3 to 23 nm) depending on the heat treatment temperature and that the porosity derived from the cumulative pore volume and true density value was 16–25%. Stathatos et al. formed a TiO_2 film on a glass substrate using CSD. Ti alkoxide was used as a raw material, and the surfactant TritonX-100 was included in the sol. The pore diameter measured using N_2 adsorption was 6–9 nm, and the pore ratio derived from the cumulative pore volume and true density value was 31–45% [23]. Choi et al. also formed a TiO_2 film on a glass substrate using CSD. Ti alkoxide was used as a raw material, and the surfactant Tween 80 was included in the sol. The pore diameter measured using N_2 adsorption was 4 nm, and the pore ratio derived from the cumulative pore volume and the true density value was 46% [24]. These data suggest that the pore diameters and porosity of films formed on substrates by CSD depend significantly on the raw materials and the coating process.

Measurement of zeta potential

Figure 6 plots the relationship between the thickness of the Al_2O_3 film deposited on SUS304L or fused silica and the measured zeta potential. The zeta potentials were nearly the same for both substrate materials and increased slightly from + 40 to + 50 mV as the thickness was increased. This indicated that the zeta potential of the coating was the same, regardless of the electrical conductivity of the substrate. Furthermore, these values were in agreement with previously reported electrophoresis data for Al_2O_3 particles [18, 19]. For comparison, the zeta potentials of bare SUS304L and fused silica substrates were plotted on the same graph as zero film thickness. These substrates were heat-treated at 773 K for 30 min, as in the case of the coated substrates. The zeta potentials of SUS304L and the fused silica substrates were approximately − 13 and − 46 mV, respectively. Fused silica had a negative potential with a larger absolute value. The zeta potential of the
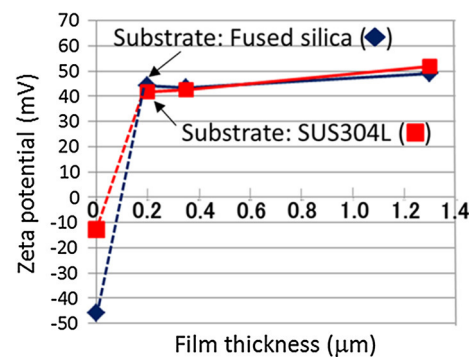
Figure 6 Relationship between film thickness and zeta potential for Al_2O_3 films coated on SUS304L and fused silica substrates (solution pH: 5.5).

fused silica substrate agreed well with the results of previously reported electrophoresis measurements on SiO$_2$ particles [20, 21].

Figure 7 shows the relationship between the number of measurements taken and the measured zeta potential for specimens with an Al$_2$O$_3$ film thickness of about 1.3 μm. Results for uncoated SUS304L and fused silica substrates are also plotted on the same graph. The number of measurements did not strongly affect the Al$_2$O$_3$-film-coated SUS304L substrate, non-coated SUS304L substrate, and non-coated fused silica substrate. On the other hand, the zeta potential clearly decreased for the Al$_2$O$_3$-coated fused silica substrate; the total decrease was about 10 mV after six measurements.

Figure 8 shows the relationship between the number of measurements taken and the measured zeta potential for specimens with the Al$_2$O$_3$ films of different thicknesses on a fused silica substrate. The zeta potential decreased with increasing number of measurements for all film thicknesses measured, namely, 0.2 μm, 0.35 μm, and 1.3 μm, and the slope of the decrease was roughly the same in each case. We proposed the following explanation for this phenomenon: The ceramic film formed by CSD typically contains continuous pores. The electrolyte solution can penetrate these pores and reach the substrate surface, producing the observed effect on the zeta potential of the substrate.

Consideration for measured zeta potential

Figure 9 is a schematic depicting the aforementioned idea. When the zeta potential is measured using the streaming potential method, the electrolyte solution is pushed into the pores of the film because of the
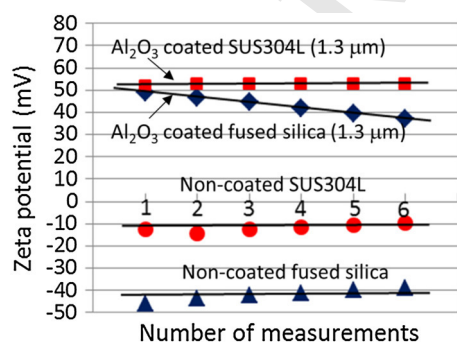

Figure 7 Relationship between number of measurements and zeta potential for Al$_2$O$_3$-film-coated and non-coated substrates (solution pH: 5.5).
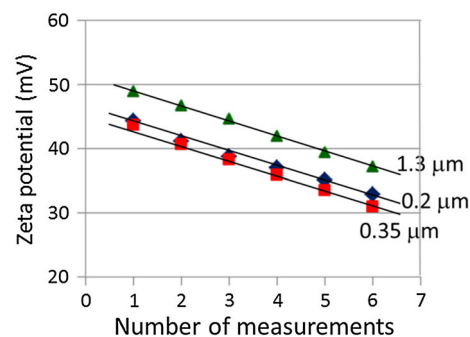

Figure 8 Relationship between number of measurements and zeta potential for Al$_2$O$_3$ films coated on fused silica substrates (solution pH: 5.5).

applied pressure. However, some of the air in the pores of the film remains. This effect was more pronounced in the Al$_2$O$_3$ film on fused silica because the zeta potential of the substrate (− 46 mV) was negative and had a large absolute value. This effect was also expected for the SUS304L substrate because in this case, a film with similar continuous pores was formed. However, the absolute value of the zeta potential of the SUS304L substrate (− 13 mV) was small, making the effect difficult to observe on this substrate.

As shown in Fig. 5a, the pore diameter in the Al$_2$O$_3$ film obtained in this study was very small at 2 nm; thus, its relationship with the hydration radius of the ions in the electrolyte was considered. Figure 10 shows the relationship between the pore diameter in the Al$_2$O$_3$ film and the hydration radius of the ions. The hydration radius of both K$^+$ and Cl$^-$ is about 0.33 nm [25]. Therefore, a maximum of three ions can be accommodated in the radial direction of the Al$_2$O$_3$ film pores. As a result, it is necessary to confirm whether the ions actually enter the pores.

Elemental analysis of K and Cl along the depth direction of Al$_2$O$_3$ film was carried out for some samples using dynamic secondary ion mass spectrometry (D-SIMS; PH16600, Physical Electronics) after zeta potential measurement. The samples were based on specimens with an approximately 1.3-μm-thick Al$_2$O$_3$ film on a fused silica substrate. The zeta potential was measured six times, after which the sample was dried in air and then further dried at 180 °C for 1.5 h in air. For comparison, similar analyses were conducted for specimens that were coated under the same conditions but were not subjected to zeta potential measurement. The primary ions used in the measurement were O$_2^-$ for K analysis and Cs$^+$

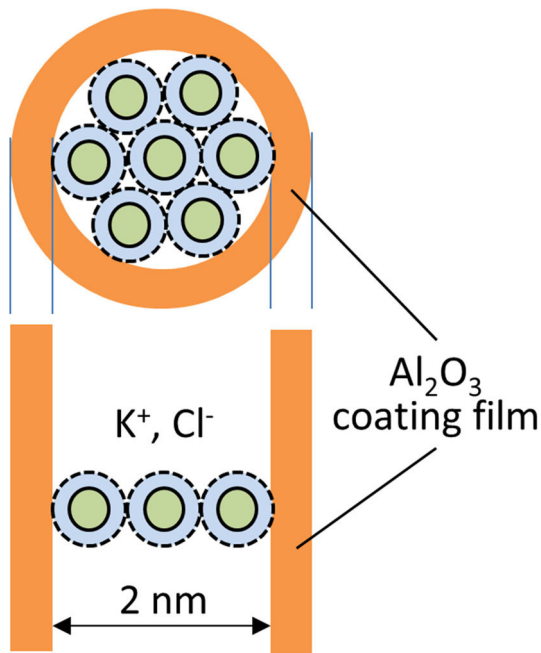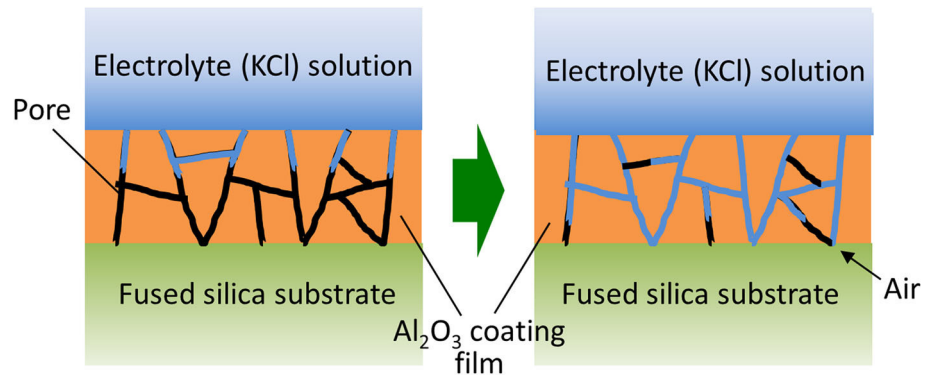**Figure 9** Infiltration of the KCl electrolyte into the pores of the Al$_2$O$_3$ film.

Figure 10 Relationship between pore diameter of Al$_2$O$_3$ film and hydration diameters of K$^+$ and Cl$^-$ ions.

402 for Cl analysis. The analysis region was located at the
403 center of the specimen, with dimensions of approxi-
404 mately 500 μm × 500 μm, and measurements were
405 conducted twice to confirm reproducibility. The
406 measurement results are given as the number of
407 atoms per number of Al$_2$O$_3$ atoms, based on the
408 predetermined standard curve.

409 Figure 11a, b shows the relationship between the
410 film depth and the K concentration of a specimen
411 before and after zeta potential measurement for
412 Al$_2$O$_3$ films with a thickness of approximately 1.3 μm
413 on a fused silica substrate, respectively. In these fig-
414 ures, the blue circles indicate K concentration in the
415 coating film. Analysis of these graphs must take into
416 account the high surface roughness of the substrate

417 (Ra of 0.4 μm) and the bilayer structure of the sam-
418 ples (substrate and film). The film depth was mea-
419 sured using a step gauge, and the horizontal axis was
420 plotted assuming a constant sputtering rate. How-
421 ever, the actual sputtering rate differs between the
422 Al$_2$O$_3$ film and fused silica substrate; thus, the hori-
423 zontal axis is only for reference. Moreover, the
424 amounts of Al and Si shown do not represent quan-
425 titative data and are only provided for reference.
426 Figure 11 shows that the concentration of K in the
427 Al$_2$O$_3$ film was about 2×10^{-5} atom% prior to zeta
428 potential measurement but increased by approxi-
429 mately two orders of magnitude to reach 2×10^{-3} -
430 atom% after the measurement. This result indicated
431 that the K$^+$ ions in the electrolyte solution penetrated
432 the pores in the Al$_2$O$_3$ film during the zeta potential
433 measurement.

434 In this case, the coated specimen appeared to have
435 a higher K concentration as the depth increased. This
436 may have been caused by the presence of K in the
437 fused silica, which is partially sputtered. Different
438 matrices containing the same concentration of K do
439 not necessarily generate the same amount of sec-
440 ondary ions in D-SIMS (matrix effect) [26]. Therefore,
441 we cannot be sure that the K concentration in Fig. 11a
442 actually increases with depth. On the other hand,
443 after zeta potential measurement, the K concentration
444 was constant up to a certain depth and then
445 decreased. Again, these values might include the
446 presence of K in the fused silica; hence, the change in
447 K concentration along the depth direction cannot be
448 discussed.

449 Figure 12a, b shows the relationship between the
450 film depth and the Cl concentration for an Al$_2$O$_3$ film
451 with a thickness of approximately 1.3 μm on a fused
452 silica substrate before and after zeta potential mea-
453 surement, respectively. In these figures, the blue

Figure 11 Relationship between film depth and K concentration for Al_2O_3 film on fused silica, evaluated by D-SIMS. **a** Before zeta potential evaluation. **b** After zeta potential evaluation.
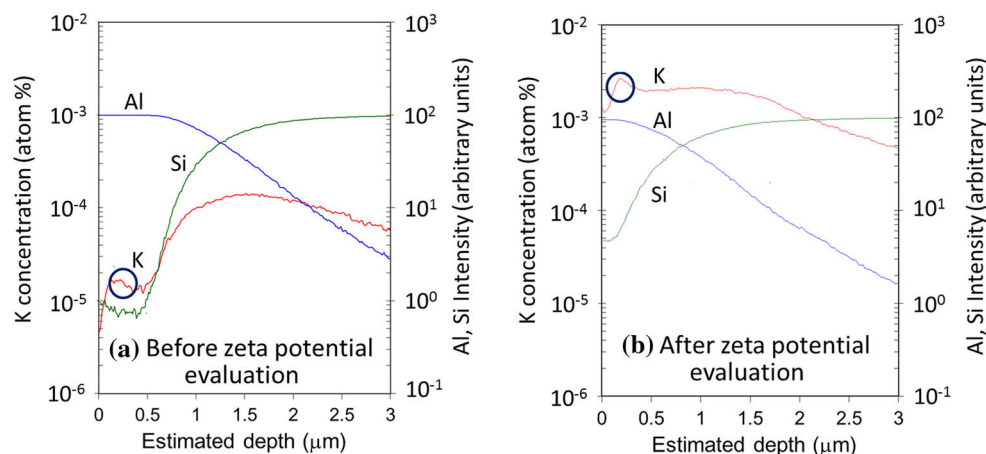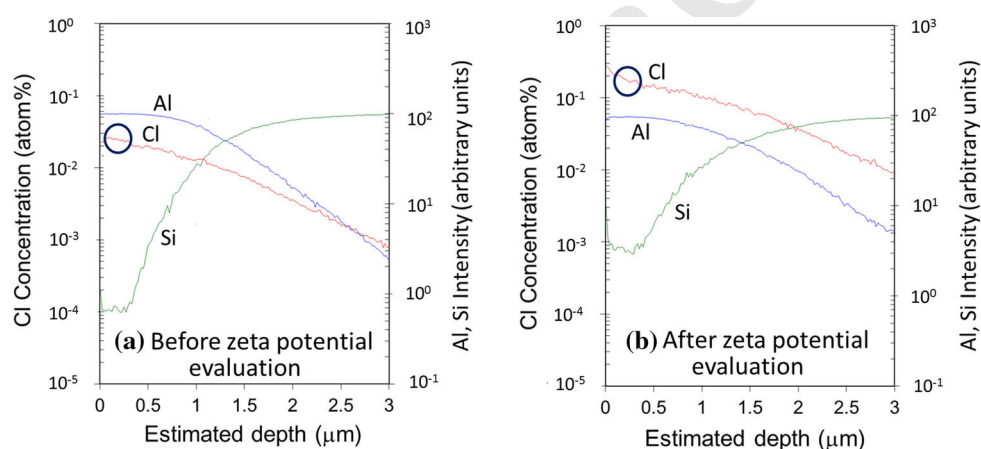

Figure 12 Relationship between film depth and Cl concentration for Al_2O_3 film on fused silica, evaluated by D-SIMS. **(a)** Before zeta potential evaluation. **(b)** After zeta potential evaluation.

454 circles indicate Cl concentration in the coating film.
455 The concentration of Cl in the specimen was about
456 2×10^{-2} atom% prior to zeta potential measurement
457 but increased by approximately one order of magni-
458 tude to 2×10^{-1} atom% after the measurement. This
459 result indicated that as with K^+, the Cl^- ions in the
460 electrolyte solution penetrated the pores in the Al_2O_3
461 film during zeta potential measurement.
462 Comparing the specimens after zeta potential
463 measurement (Figs. 11b, 12b), the concentrations of
464 K^+ and Cl^- ions were about 2×10^{-3} atom% and
465 2×10^{-1} atom%, respectively; that is, the concentra-
466 tion of Cl^- was approximately 100 times that of K^+. A
467 possible explanation for this difference is that the
468 positive zeta potential of the surfaces of the pores in
469 the Al_2O_3 film at pH 5.5 [18, 19] facilitates the pene-
470 tration of the oppositely charged Cl^- ions.
471 If the hypothesis in Fig. 9 is correct, a specimen
472 impregnated with the KCl electrolyte solution under
473 vacuum (to remove the remaining air in the pores)
474 should exhibit a constant zeta potential, even after

475 repeated measurements. Therefore, zeta potential
476 measurements were conducted after vacuum
477 impregnation of KCl electrolyte solution into the
478 coating specimen by the streaming potential method.
479 The vacuum impregnation method is shown in
480 Fig. 13. An Al_2O_3 film with a thickness of 1.3 μm was
481 coated onto a fused silica substrate, which was held
482 in a PP container. The entire vacuum chamber
483 including PP container was evacuated for 30 min
484 using a rotary pump. Then, 1 mM KCl solution was
485 injected into the PP container. Evacuation was con-
486 tinued for another 10 min; then, the vacuum was
487 released so that the chamber reached atmospheric
488 pressure. The PP container holding the specimen was
489 removed from the vacuum chamber, and a lid was
490 placed on the container. After the specimen was
491 allowed to rest for 120 h, the zeta potential was
492 measured. Figure 14 shows the relationship between
493 the number of measurements and the measured zeta
494 potential. The zeta potential after vacuum impreg-
495 nation was constant at approximately 32 mV and did

Figure 13 Conceptual scheme of the vacuum impregnation process for the Al$_2$O$_3$-coated fused silica specimen.
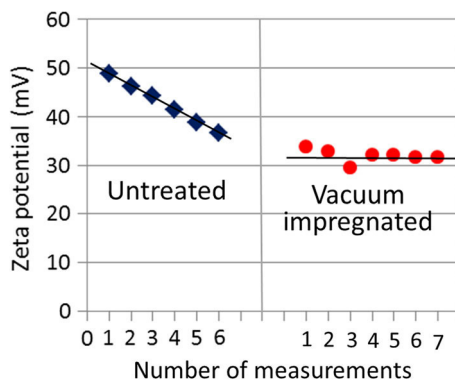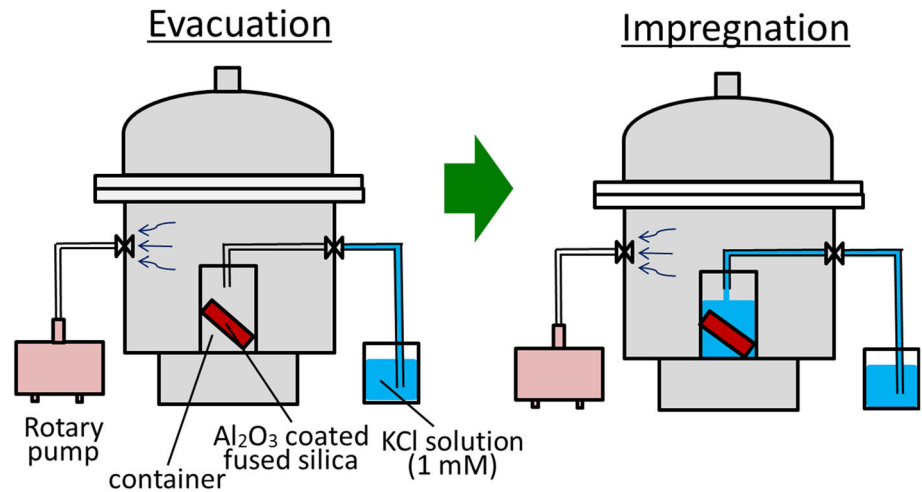

Figure 14 Relationship between number of measurements and zeta potential for untreated and vacuum-impregnated Al$_2$O$_3$ films coated on fused silica (film thickness: 1.3 μm).

Figure 15 Mechanism of reduction in the zeta potential for Al$_2$O$_3$ film coated on fused silica substrate.

not depend on the number of measurements performed. Therefore, the decrease in the zeta potential with repeated measurements in Fig. 8 was due to the fact that the KCl solution gradually penetrated the Al$_2$O$_3$ film.

Figure 15 depicts the mechanism of the decrease in the zeta potential that is implied from the experimental results above. The K$^+$ and Cl$^-$ ions in the electrolyte penetrate the pores in Al$_2$O$_3$ due to the pressurization during the zeta potential measurement. This penetration is gradual because some air remains in the Al$_2$O$_3$ pores. Cl$^-$ ions are attracted to the pores at the surface of the Al$_2$O$_3$ film, which has a positive zeta potential, and form a fixed bed. In contrast, K$^+$ ions are attracted to the surface of the fused silica substrate, which has a negative zeta potential, and form an electrical double layer. As a result, a region in which K$^+$ ions are depleted (depletion lay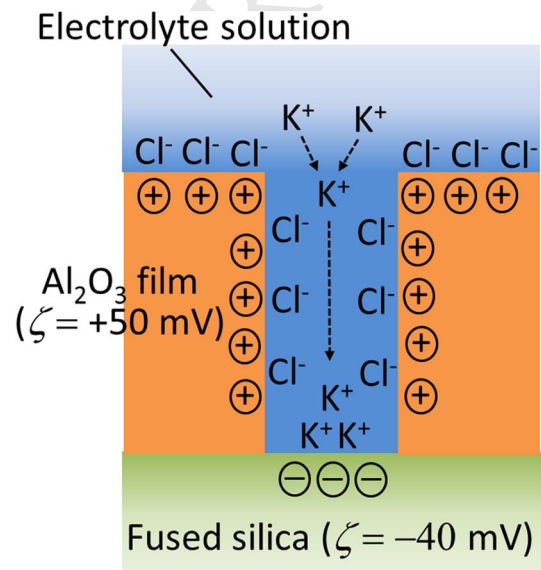er) is formed on the surface side of the electrical double layer (upper side of Fig. 15). In consequence, the K$^+$ ions diffuse from the electrolyte solution existing outside of the pores in the Al$_2$O$_3$ film into this depletion layer, causing the region near the Al$_2$O$_3$ film surface to become K$^+$-rich, and the anion concentration decreases. The zeta potential measured using the streaming potential method should correspond to the total charge of the ions near the surface of the Al$_2$O$_3$ film, and thus, the zeta potential decreases when the electrolyte solution penetrates the pores of the film.

Conclusions

Al₂O₃ films were coated on SUS304L stainless steel and fused silica substrates using CSD, and the continuous pores with a diameter of approximately 2 nm were observed in the films. The zeta potential of the film was measured using the streaming potential method. Initially, the measured zeta potential of the Al₂O₃ films was + 40 to + 50 mV, which was the same for both substrates. However, the zeta potential of the Al₂O₃ film on the fused silica substrate decreased significantly with repeated measurements. It was considered that electrolyte solution penetrated these pores and reached the fused silica substrate, and thus, the zeta potential of the fused silica substrate gradually affected the measured zeta potential. This is a characteristic phenomenon that occurs when the zeta potential of a film containing continuous pores is measured using the streaming potential method. The streaming potential method is a superior measurement method by which the zeta potential of a film coated on a metal substrate can be measured. However, when measuring a film with continuous pores, it is necessary to pay attention to the facts found in this study.

Acknowledgements

Compliance with ethical standards

Conflict of interest   There authors declare that they have no conflict of interest.

References

[1] Kim YJ, Dulka C (2008) Oxide fouling mitigation technology in BWR. In: Proceedings of the 2008 international congress on advances in nuclear power plants (ICAPP' 08), pp 2142–2150

[2] Dulka CP, Blake F, Lenz M, Bass J, Perry V, Ross R (2008) A novel fouling mitigation method for jet pump inlet mixers. In: Proceedings of the 10th NRC/ASME symposium on valves, pumps and inservice testing, pp 1A:3–1A:12

[3] Watanabe M, Sayano A, Kinugasa K, Mori H, Hagiwara T (2013) Improvement of jet pump mixer in boiling water reactor for mitigating flow-induced vibration and fouling. In: Proceedings of the ASME 2013 pressure vessels and piping conference (PVP2013), pp PVP2013–97235

[4] Kuo RJ, Matijevic E (1980) Particle adhesion and removal in model systems: III. Monodispersed ferric oxide on steel. J Colloid Interface Sci 78:407–421

[5] Jayaweera P, Hettiarachchi S, Ocken H (1994) Determination of the high temperature zeta potential and pH of zero charge of some transition metal oxides. Colloids Surf A Physicochem Eng Asp 85:19–27

[6] Sayano A, Saito N, Kaneko T, Okamura M, Yamazaki K, Morishima Y, Mori H (2012) Development of sol–gel coating process for preventing adhesion of iron oxides. In: Proceedings of the 55th Japan congress on materials research, vol 512, pp 248–249

[7] Sayano A, Kanno H, Inagaki S, Takahashi M, Yoshida M (2015) The formation of Cr(VI) compound at the interface between metal and heat-insulating material and the approach to prevent the formation by sol–gel process. J Ceram Soc Jpn 123:677–684

[8] Ono S, Nishi Y (2001) Chromium-free corrosion resistance of metals by ceramic coating. J Am Ceram Soc 84:3054–3056

[9] Tiwari SK, Mishra T, Gunjan MK, Bhattacharyya AS, Singh TB, Singh R (2007) Development and characterization of sol–gel silica–alumina composite coatings on AISI 316L for implant applications. Surf Coat Technol 201:7582–7588

[10] Sayano A, Tazawa T, Yan L, Takahashi M, Okuno K, Murakami I (2016) Suppression of oxidation of high chromium steels at elevated temperatures in steam atmosphere by alumina-based coating film grown by chemical solution deposition process. J Ceram Soc Jpn 124:448–454

[11] Brinker CJ, Frye GC, Hurd AJ, Ashley CS (1991) Fundamentals of sol–gel dip coating. Thin Solid Films 201:97–108

[12] Kitahara F, Furusawa K, Ozaki M, Oshima H (1995) Zeta potential. Scientist Press Co., LTD, Beijing, pp 75–79

613 [13] Wu SF, Yanagisawa K, Nishizawa T (2001) Zeta potential of
614   conductive plates: (I) development of a zeta potential
615   determination method. Surf Sci Soc Jpn 22:504–509

616 [14] Lorenzetti M, Luxbacher T, Kobe S, Novak S (2015) Elec-
617   trokinetic behaviour of porous TiO_2-coated implants. J Mater
618   Sci 26:191–194. https://doi.org/10.1007/s10856-015-5521-4

619 [15] Daiguji H (2005) Transport phenomena in nanofluidic
620   channels. J Surf Finish Soc Jpn 56:913–918

621 [16] Yaroshchuk A, Luxbacher T (2010) Interpretation of elec-
622   trokinetic measurements with porous films: role of electric
623   conductance and streaming current within porous structure.
624   Langmuir 26:10882–10889

625 [17] Barrett EP, Joyner LG, Halenda PP (1951) Study of pore size
626   distribution by capillary absorption method. J Am Chem Soc
627   73:373–380

628 [18] Valdivieso AL, Bahena JLR, Song S, Urbina RH (2006)
629   Temperature effect on the zeta potential and fluoride
630   adsorption at the α-Al_2O_3/aqueous solution interface. J Col-
631   loid Interface Sci 298:1–5

632 [19] Leong YK, Ong BC (2003) Critical zeta potential and the
633   Hamaker constant of oxides in water. Powder Technol
634   134:249–254

635 [20] Tseng WJ, Tsai P, Lin TE (2010) Electrophoretic movement
636   of hollow silica particles under DC electric fields. J Ceram
637   Soc Jpn 118:309–313

638 [21] Lee D, Omolade D, Cohen RE, Rubner MF (2007) pH-
639   dependent structure and properties of TiO_2/SiO_2 nanoparticle
640   multilayer thin films. J Chem Mater 19:1427–1433

641 [22] Guo P, Aegerter MA (1999) RU(II) sensitized Nb_2O_5 solar
642   cell made by the sol–gel process. Thin Solid Films
643   351:290–294

644 [23] Stathatos E, Lianos P, Tsakiroglou C (2004) Highly efficient
645   nanocrystalline titania films made from organic/inorganic
646   nanocomposite gels. Microporous Mesoporous Mater
647   75:255–260

648 [24] Choi H, Stathatos E, Dionysiou DD (2006) Sol–gel prepa-
649   ration of mesoporous photocatalytic TiO_2 films and TiO_2/
650   Al_2O_3 composite membranes for environmental applications.
651   Appl Catal B 63:60–67

652 [25] Israelachvili J (1992) Intermolecular and surface force, 2nd
653   edn. Academic Press, London, pp 41–44

654 [26] Miwa S (1996) Secondary ion mass spectrometry. Bunseki
655   8:596–602